Future Cosmic Microwave Background delensing with galaxies surveys.

A. Manzotti[1, 2, *]

[1] *Kavli Institute for Cosmological Physics, University of Chicago,*
5640 South Ellis Avenue, Chicago, IL 60637, USA
[2] *Department of Astronomy and Astrophysics, University of Chicago,*
5640 South Ellis Avenue, Chicago, IL 60637, USA

(Dated: May 11, 2017)

- Worry : they might ask for internal bias item Possible TODO : temperature N_{eff}

The measurement of the CMB polarization is a promising experimental dataset to test the inflationary paradigm and to probe the physics of the early universe. A particular component, the so called B-modes is indeed a direct signature of the presence of gravitational waves in the early universe. However improving the level of noise is not enough. This is even more true if the aim is to not only detect the amplitude of gravitational waves but also the shape of their spectrum to test for example inflation consistency relations. Removing the lensing component from the measurement of CMB B-modes will be important to constraint the amplitude of the primordial gravitational wave contribution to the signal. Here we discuss the role of current and future large scale structure surveys in improving the reconstruction of the lensing potential that lenses the CMB photons. We find that..

I. INTRODUCTION

Inflation Physics with CMB
Current constraints
Now limiting by delensing
Done what are the prospects/
This paper is organized as follow:

II. GRAVITATIONAL LENSING B-MODE

As for the CMB photons temperature, the intensity map of photons on the sky, also the Q and U mode decomposition of their polarization is remapped by lensing as:

$$Q(\hat{\mathbf{n}}) = Q_{\text{unlensed}}(\hat{\mathbf{n}} + \nabla\phi); \quad U(\hat{\mathbf{n}}) = U_{\text{unlensed}}(\hat{\mathbf{n}} + \nabla\phi) \tag{1}$$

where $\nabla\phi$ is the deflection angle directly related to the lensing potential potential integrated along the line of sight ϕ. The CMB polarization is usually decompose into odd-parity Fourier modes E and B. As shown in [] this for symmetry reason the B-modes configuration is mainly sourced by tensor perturbations. However this promising sign of primordial gravitational waves is partially obscured by a secondary mechanism that can produce B-modes in the late universe. Indeed gravitational interaction with large scale structure generates CMB B-modes by distorting primordial E-modes.

As a first approximation, given a convergence field $\kappa = -\frac{1}{2}\nabla^2\phi$ the B mode resulting from the lensing of primordial E mode is:

$$B^{\text{lens}}(\mathbf{l}) = \int \frac{d^2\mathbf{l}'}{(2\pi)^2} W(\mathbf{l}, \mathbf{l}') E(\mathbf{l}') \kappa(\mathbf{l} - \mathbf{l}') \tag{2}$$

where different modes contributes with a different weight given by:

$$W(\mathbf{l}, \mathbf{l}') = \frac{2\mathbf{l}' \cdot (\mathbf{l} - \mathbf{l}')}{|\mathbf{l} - \mathbf{l}'|^2} \sin(2\varphi_{\mathbf{l}, \mathbf{l}'}), \tag{3}$$

As usual we define the power spectrum as:

$$\langle B^{\text{lens}}(\mathbf{l}) \, B^{\text{lens}^*}(\tilde{\mathbf{l}}) \rangle \equiv (2\pi)^2 \delta^D(\mathbf{l} - \tilde{\mathbf{l}}) C_l^{BB,\text{lens}} \tag{4}$$

From this we get that the power spectrum of the lensing component of the B-modes:

$$C_l^{BB,\text{lens}} = \int \frac{d^2\mathbf{l}'}{(2\pi)^2} W^2(\mathbf{l}, \mathbf{l}') C_{l'}^{EE} C_{|\mathbf{l}-\mathbf{l}'|}^{\kappa\kappa}. \tag{5}$$

The full B-mode power spectrum measured on the sky is given by a possible primordial component $C_l^{BB,r}$ together with the lensing $C_l^{BB,\text{lens}}$ contribution and instrumental noise N_l^{BB}:

$$C_l^{BB,\text{full}} = C_l^{BB,r} + C_l^{BB,\text{lens}} + N_l^{BB}. \tag{6}$$

Given the current constrains, the lensing component is a significant source of B-modes that, for GW searches purposes correspond to a white noise source of roughly $5\mu K$-arcmin. This means that it is not only bigger than the biggest allowed GW contribution at scale bigger than several degrees but it is comparable with the decreasing level of instrumental noise. For this reason it is very important to characterize it and eventually remove it form the data. This can be done for example using Eq. (2) (or its real-space analogue) given a measurement of the E-mode field and the lensing potential ϕ. While E is measured directly, we ca estimate ϕ using "tracers" of the dark matter distribution that creates the potential.

If we have a large scale structure field $I(\hat{\mathbf{n}})$ that traces the lensing potential responsible for the lensing of the

---

CMB the template of the lensing B mode on the sky is a weighted convolution:

$$\hat{B}^{\text{lens}}(\mathbf{l}) = \int \frac{d^2\mathbf{l}'}{(2\pi)^2} W(\mathbf{l}, \mathbf{l}') f(\mathbf{l}, \mathbf{l}') E^N(\mathbf{l}') I(\mathbf{l} - \mathbf{l}') \quad (7)$$

where $f(\mathbf{l}, \mathbf{l}')$ can be determined minimizing the difference with the true $B^{\text{lens}}(\mathbf{l})$ defined in Eq. (2).

The residual lensing B mode due to an imperfect knowledge of the true E-mode and ϕ will be

$$B^{\text{res}}(\mathbf{l}) = B^{\text{lens}}(\mathbf{l}) - \hat{B}^{\text{lens}}(\mathbf{l}) = \int \frac{d^2\mathbf{l}'}{(2\pi)^2} W(\mathbf{l}, \mathbf{l}') \times$$
$$\left(E(\mathbf{l}')\kappa(\mathbf{l} - \mathbf{l}') - f(\mathbf{l}, \mathbf{l}') E^N(\mathbf{l}') I(\mathbf{l} - \mathbf{l}') \right) \quad (8)$$

The weights $f(\mathbf{l}, \mathbf{l}')$ so that the residual lensing B mode power is minimized are:

$$f(\mathbf{l}, \mathbf{l}') = \left(\frac{C_{l'}^{EE}}{C_{l'}^{EE} + N_{l'}^{EE}} \right) \frac{C_{|\mathbf{l}-\mathbf{l}'|}^{\kappa I}}{C_{|\mathbf{l}-\mathbf{l}'|}^{II}} \quad (9)$$

Notice that the first term consists in the usual inverse variance filter applied to the measured E-mode and the second minimize the difference between the reconstructed ϕ and the CMB lensing potential.

With this choice of $f(\mathbf{l}, \mathbf{l}')$ we finally have that the residual power is:

$$C_l^{BB,\text{res}} = \int \frac{d^2\mathbf{l}'}{(2\pi)^2} W^2(\mathbf{l}, \mathbf{l}') C_{l'}^{EE} C_{|\mathbf{l}-\mathbf{l}'|}^{\kappa\kappa} \quad (10)$$
$$\times \left[1 - \left(\frac{C_{l'}^{EE}}{C_{l'}^{EE} + N_{l'}^{EE}} \right) \rho_{|\mathbf{l}-\mathbf{l}'|}^2 \right]$$

with

$$\rho_l = \frac{C_l^{\kappa I}}{\sqrt{C_l^{\kappa\kappa} C_l^{II}}}. \quad (11)$$

The bigger ρ_l is for a LSS field the more it is correlated with the lensing potential acting on the CMB photons. An higher correlation allows for a better reconstruction of the ϕ^{CMB} and, as a consequence, of B^{lens}.

A. Multiple tracers of the lensing potential

Let's now assume that we have n different tracers of the gravitational potentials I_i with $i \in \{1, .., n\}$. It can be shown that the optimal way to combine them to estimate ϕ or, in other word, maximizing the correlation factor ρ is:

$$I = \sum_i c^i I^i$$
$$c_i = (C^{-1})_{ij} C^{\kappa I^j} \quad (12)$$

where C is the covariance matrix of the LSS tracers. The "effective" correlation of these combined tracers with gravitational lensing is:

$$\rho^2 = \sum_{i,j} \frac{C^{\kappa i} (C^{-1})_{ij} C^{\kappa j}}{C^{\kappa\kappa}}. \quad (13)$$

Note that gain we have in adding a new tracer is not only proportional to its correlation with the CMB lensing but it also depends on how much it is correlated with the already used set of tracers. Fig. 1 show the different kernels as a function of redshift computed using the models and parameters described in the following sections. Galaxies clustering surveys can only reconstruct the low-z portion of the lensing kernel as can be seen from the LSST DES and DESI curves. However given the significant low noise of this measurement they can still help the delensing of the CMB. Furthermore the low-redshift tail of the lensing kernel is also the one affected by large scale structures non-linearities. They can indeed be extremely helpful if future CMB surveys will try to remove that contribution instead of attempting to model it. On the other hand CIB and 21 cm surveys are target to high redshift structures and independently from the model assumed they show a fairly good overlap with the CMB lensing kernel.
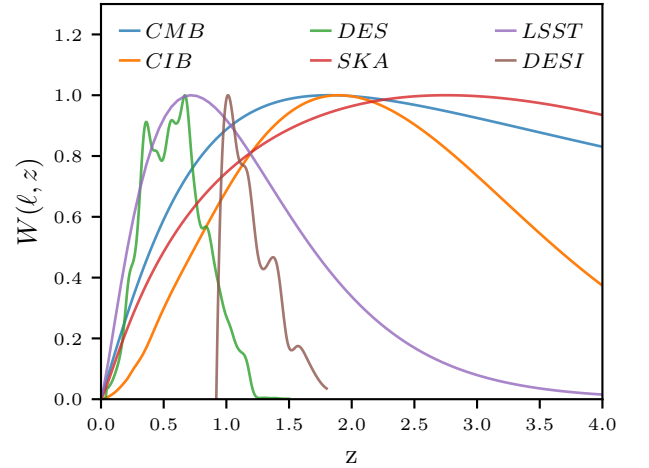

FIG. 1. Comparison of the different kernels used in this analysis. The bigger the overlap wit the CMB lensing kernel the better the reconstruction of the lensing potential will be. This will lead to a better delensing.

III. TRACERS MODEL

In this section we briefly describe how the power spectra of section II are computed and what it is assumed for the different tracers considered in this work.

A 2D projected field δ^i that traces dark matter over-densities can be seen as a 3D field projected along the line of site as:

$$\delta^i(\hat{\mathbf{n}}) = \int_0^\infty dz \, W^i(z)\delta(\chi(z)\hat{\mathbf{n}}, z). \quad (14)$$

where $\delta(\chi(z)\hat{\mathbf{n}}, z)$ correspond to the dark matter overdensity field at a comoving distance $\chi(z)$ at redshift z in the angular direction $\hat{\mathbf{n}}$. Using the Limber approximation [8] we can compute the power spectra of 2 fields i, j as:

$$C_\ell^{ij} = \int_0^\infty \frac{dz}{c} \frac{H(z)}{\chi(z)^2} W^i(z) W^j(z) P(k, z). \qquad (15)$$

In this equation, $H(z)$ is the Hubble factor at redshift z, c is the speed of light, $\chi(z)$ the comoving distance $P(k, z)$ is the matter power spectrum evaluated at wavenumber $k = \ell/\chi(z)$ at redshift z. Furthermore $W^i(z)$ is the kernel function of the field i. These theoretical quantities have been computed using CAMB and HALOFIT.

A. CMB lensing potential

CMB photons interact gravitationally with low-redshift large scale structure. The deflection angle is given by $\mathbf{d}(\hat{\mathbf{n}}) = \nabla\phi(\hat{\mathbf{n}})$, where ∇ is the the two-dimensional gradient on the sphere. Because the lensing potential is an integrated measure of the projected gravitational potential, taking the two-dimensional Laplacian of the lensing potential we can define the lensing convergence $\kappa(\hat{\mathbf{n}}) = -\frac{1}{2}\nabla^2\phi(\hat{\mathbf{n}})$, which depends on the projected matter overdensity δ The lensing kernel W^κ is $\chi(z)$ is the comoving distance to redshift z, χ_* is the comoving distance to the last-scattering surface at $z_* \simeq 1090$

$$W^\kappa(z) = \frac{3\Omega_{\rm m}}{2c} \frac{H_0^2}{H(z)} (1+z)\chi(z) \frac{\chi_* - \chi(z)}{\chi_*}, \qquad (16)$$

where $\Omega_{\rm m}$ and H_0 are the present day values of the Hubble and matter density parameters, respectively.

The CMB lensing potential is *the* field that we need to reconstruct in order to reverse the effect of large scale structure and delens the CMB. However the lensing potential can also be reconstructed from the CMB itself. In that case it can be see as a noisy tracer of the true field. While the CMB internal reconstruction fiels as the same kernel as the true one $W^\kappa(z)$. Given the instrumental noise level and the beam, we can compute the reconstruction noise $N_l^{\kappa\kappa}$, so that its power spectrum is

$$C_l^{\kappa_{\rm rec}\kappa_{\rm rec}} = C_l^{\kappa\kappa} + N_l^{\kappa\kappa} \qquad (17)$$

In this work the level of noise is computed assuming an iterative quadratic estimator is used in the reconstruction.

B. Galaxies

The galaxy overdensity $g(\hat{\mathbf{n}})$ in a given direction on the sky is also expressed as a line of sight integral of the matter overdensity:

$$g(\hat{\mathbf{n}}) = \int_0^{z_*} dz\, W^g(z)\delta(\chi(z)\hat{\mathbf{n}}, z), \qquad (18)$$
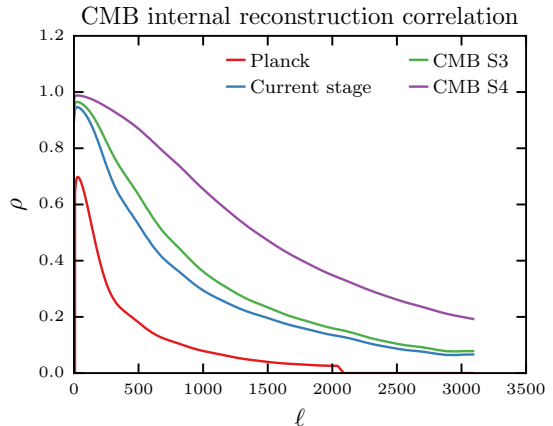
3

FIG. 2. **CMB alone:** Correlation factor between CMB internal reconstructed potential and the true lensing potential for different CMB experiments and corresponding noise reconstructions.

where the kernel is

$$W^g(z) = \frac{b(z)\frac{dN}{dz}}{\left(\int dz' \frac{dN}{dz'}\right)}. \qquad (19)$$

Here $\frac{dN}{dz}$ is the number of galaxies as a function of redshift observed by the survey while $b(z)$ is the galaxy bias that connect at different redshift the amplitude of galaxies overdensity to the one of the dark matter. When computing the auto-spectrum of a galaxies density the shot noise term needs to be taken into account. This is done by adding a constant term to the power spectrum equal to the inverse of the number of galaxies per steradians.

Different galaxy surveys in this work are fully characterized by their b(z), $\frac{dN}{dz}$ and the observed galaxies density. We test the delensing efficiency modelling current survey like WISE or D.E.S as well as future galaxy probes like D.E.S.I LSST together with 21 cm measurement like SKA.

WISE redsfhit distribution is taken from DES is modeled usin For DESI we used the ..
LSST is model following
We model SKA following

C. Cosmic infrared Background

The definition of the kernel of the CIB is more complex and model dependent. Following [?], we model the CIB power directly as $C_\ell^{\rm CIB\text{-}CIB} = 3500(l/3000)^{-1.25}\,{\rm Jy}^2/{\rm sr}$. This model provides an accurate fit for the power of the *Herschel* $500\,\mu$ map used in this work. For the cross-spectra with the CMB lensing or other galaxies tracers $C_\ell^{\rm CIB\text{-}j}$, we use the single-SED model of [4]. This places the peak of the CIB emissivity at redshift $z_c = 2$ with

a broad redshift kernel of width $\sigma_z = 2$. This model is rescaled to agree with the results of **?**] and **?**] by choosing the corresponding linear bias parameter. Other multi-frequency CIB models are available [e.g., **?**]; however, given the level of noise, we are relatively insensitive to this choice. With these assumptions, depending on angular scale, $45-65\%$ of the CIB is correlated with the CMB lensing potential, as shown in Fig. 4. [1–3, 5–7, 10–15]

IV. FORECAST

In this section we forecast the expected delensing efficiency and the relative importance of galaxies tracers for current and future experiments. We focus on 3 different scenarios: the current stage, the 3G one and the futuristic CMB Stage 4.

A. Fisher method

We defined the B-modes noise spectrum:

$$N_l^{BB} = (\Delta_P/T_{\rm CMB})^2 \, e^{l^2 \theta^2_{\rm FWHM}/(8 \ln 2)} \qquad (20)$$

where $\theta_{\rm FWHM}$ is the full half width of the telescope beam and Δ_P is the instrumental noise of the experiment. The gaussian covariance is then:

$$\sigma(C_l^{BB,\rm full}) = \sqrt{\frac{2}{(2l+1)f_{\rm sky}}} \left(C_l^{BB,\rm lens} + N_l^{BB} \right). \quad (21)$$

With this we can simply quantify the constraints on the tensor to scalar ration r:

$$\sigma(r) = \left[\sum_l \frac{\left(\frac{\partial C_l^{BB,r}}{\partial r}\right)^2}{\sigma^2(C_l^{BB,\rm full})} \right]^{-\frac{1}{2}} \qquad (22)$$

$$\approx \left[\frac{\sum_l (2l+1)f_{\rm sky}\left(\frac{\partial C_l^{BB,r}}{\partial r}\right)^2}{2} \right]^{-\frac{1}{2}} \langle C_l^{BB,\rm lens} + N_l^{BB} \rangle_{l<100}$$

where to go from the first to the second line we use the fact that most of the constraint comes from large scale modes at $\ell < 100$, thus larger mode can be ignore here. We quantify the improvement due to delensing as the factor α defined as the ration of the error before and after delensing:

$$\alpha = \frac{\langle C_l^{BB,\rm lens} + N_l^{BB}[\Delta_P] \rangle_{l<100}}{\langle C_l^{BB,\rm res}[\Delta_P] + N_l^{BB}[\Delta_P] \rangle_{l<100}} \qquad (23)$$

B. Current generation

Very recently delensing has been proven possible on real data using both the internal CMB lensing potential

reconstruction as well as external tracers. Here we discuss the improvement due to combining this two probes. This is already possible both on full sky using Planck data or in smaller sky patches combining Herschel or Planck CIB data with SPT and BK data. Furthermore we test how much current relative low redshift galaxies surveys like D.E.S can improve delensing efficiency on smaller patch of the sky like the Bicep-Keck SPT-Pol footprint.

We model the current generation pf CMB experiments after 3 experiments: a full sky Planck experiment together with a deep low noise experiemtn and a high resolution one on a smaller patch of the sky.

The correlation attainable using current experiments is shown in Fig. 4.

At large angular scale the CMB internal reconstruction is clearly the best tracers for delensing. Because of the large level of noise in current experiment, its efficiency became comparable to the CIB one at few degrees ($\ell \simeq 400$).
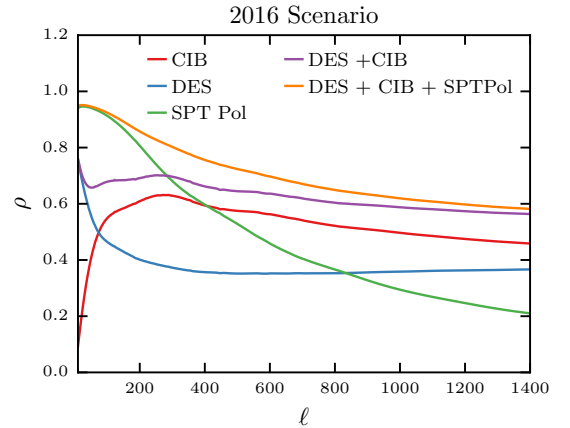
TABLE I. α: Current generation improvements

Surveys	α
des	1.34
cib	1.71

FIG. 3. Correlation factor between current galaxies survey and internally reconstructed ϕ CMB lensing potential as a function of the multipole ℓ.

C. CMB-S3 Era

The accuracy of CMB is rapidly improving. For example the next generation of the SPT telescope, SPT3G has been deployed and is currently taking data. Furthermore other experiments have considerably increased the number of detectors (AdvACT etc.). We will assume a level
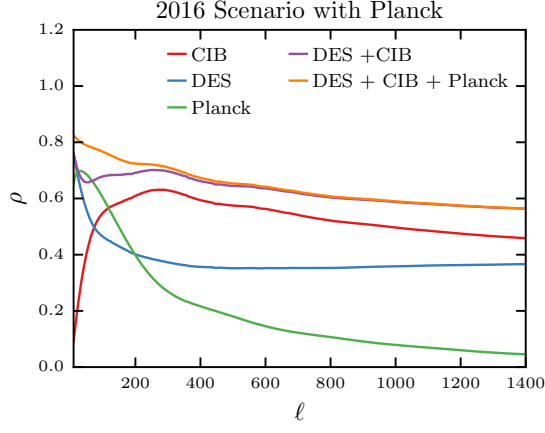
FIG. 4. Correlation factor between current galaxies survey and internally reconstructed ϕ CMB lensing potential as a function of the multipole ℓ.

TABLE II. α: Stage-3 improvements

Surveys	α
des	1.34
cib	1.71

of noise of 3 μK-arcmin the level predicted for SPT3G. The correlation attainable using current experiments is shown in Fig. 5,
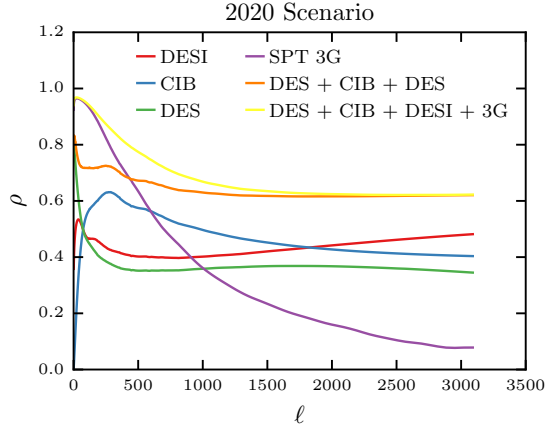

FIG. 5. Correlation factor. Same as Fig. 4 but for stage 3 experiments.

D. CMB-S4 Era

An ambitious program for a generation 4 ground CMB experiment is currently under planning. Moreover satel-

TABLE III. α: Stage-4 improvements

Surveys	α
des	1.34
cib	1.71

lite experiments have been proposed.

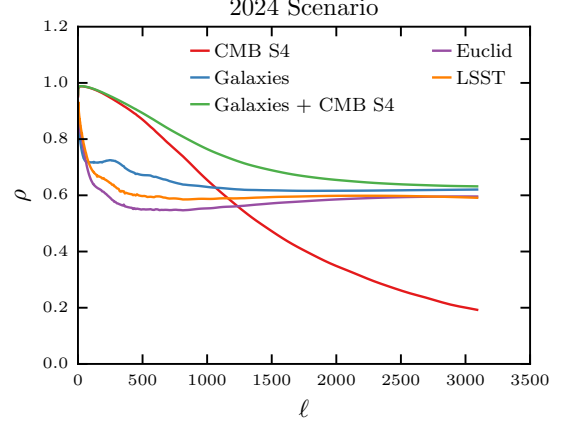The correlation attainable using current experiments is shown in Fig. 6,

FIG. 6. Correlation factor. Same as Fig. 4 but for stage 4 experiments.

E. Bias uncertainties degradation

The uncertainties in the theoretical assumptions used to model the galaxies can cause a degradation of the improvement of inflationary constraint of delensed spectra. In this section we quantify this effect. We will now marginalize over unknown galaxies parameters but we will use a full dataset of CMB and galaxies data. The idea is that as shown in the low level of noise in galaxies surveys might allow us to internally calibrate them. We will use a Fisher approach the Fisher matrix is:

$$F_{pq} = \sum_{l_a=l_{\min}^{BB}}^{l_{\max}^{BB}} \sum_{l_b=l_{\min}^{BB}}^{l_{\max}^{BB}} \frac{\partial C_{l_a}^{BB,\mathrm{del}}}{\partial \theta_p} \left[\mathrm{Cov}^{BB,BB}\right]_{l_a,l_b}^{-1} \frac{\partial C_{l_b}^{BB,\mathrm{del}}}{\partial \theta_q}$$
$$+ \sum_j \frac{\frac{\partial C_j^{\kappa I}}{\partial \theta_p} \frac{\partial C_j^{\kappa I}}{\partial \theta_q}}{(\Delta C_j^{\kappa I})^2} + \sum_j \frac{\frac{\partial C_j^{II}}{\partial \theta_p} \frac{\partial C_j^{II}}{\partial \theta_q}}{(\Delta C_j^{II})^2} \quad (24)$$

$$\alpha_{\mathrm{marginalized}} = \sigma_0(r)/\sigma_{\mathrm{marginalized/delensed}}(r) \quad (25)$$

where the parameter array contains both the tensor to scalar rate $\theta = r$, and the galaxies surveys parameters like the bias b_i or p_i [9].

TABLE IV. α: improvement on r constraint

Surveys	α
des	1.34
cib	1.71
cmb current	1.79
gals current	2.03
cmb S3	2.15
gals S3	2.16
gals S4	2.16
comb current	2.66
comb S3	3.14
cmb S4	4.36
comb S4	5.27

We compute the derivatives of the power spectra as described

V. CONCLUSIONS

Delensing or more in general the ability to separate the lensing component of the B-mode from a possible primordial inflationary signal is crucial to fully exploit the capabilities of future experiments. In this paper we studied the possible impact of large scale structure surveys in this important endeavor. For current experiment CIB data had already proven to be very efficient in delensing. If no High res experiment is avaiable to reconstruct the lensing potential phi even a low-z experiment like D.E.S will improve th delensign efficiency by 10% if combined with Planck lensing and a CIB tracers. As expected the lower the noise in the CMB experiment the more the delensign efficiency will be predominately come from the internal CMB reconstruction of the lensing potential. Indeed using the CMB itself we reconstruct only the lenses that actually lens the CMB obtained an almost perfect cleaning in the absence of noise. This approach will need a careful study of possible biases coming from using the same source (the CMB) we are delensing to reconstruct the lensing effect itself. This has already been applied to data and studied. However the fairly good efficiency of galaxies tracers might come in end to cross-check these internal biases. This will probably be needed to confirm a possible detection of gravitation waves if this rely heavily on delensing.

VI. ACKNOWLEDGMENTS

[1] P. A. R. Ade, R. W. Aikin, D. Barkats, S. J. Benton, C. A. Bischoff, J. J. Bock, J. A. Brevik, I. Buder, E. Bullock, C. D. Dowell, L. Duband, J. P. Filippini, S. Fliescher, S. R. Golwala, M. Halpern, M. Hasselfield, S. R. Hildebrandt, G. C. Hilton, V. V. Hristov, K. D. Irwin, K. S. Karkare, J. P. Kaufman, B. G. Keating, S. A. Kernasovskiy, J. M. Kovac, C. L. Kuo, E. M. Leitch, M. Lueker, P. Mason, C. B. Netterfield, H. T. Nguyen, R. O'Brient, R. W. Ogburn, A. Orlando, C. Pryke, C. D. Reintsema, S. Richter, R. Schwarz, C. D. Sheehy, Z. K. Staniszewski, R. V. Sudiwala, G. P. Teply, J. E. Tolan, A. D. Turner, A. G. Vieregg, C. L. Wong, K. W. Yoon, and Bicep2 Collaboration. Detection of B-Mode Polarization at Degree Angular Scales by BICEP2. *Physical Review Letters*, 112(24):241101, June 2014.

[2] F. Boulanger, A. Abergel, J.-P. Bernard, W. B. Burton, F.-X. Desert, D. Hartmann, G. Lagache, and J.-L. Puget. The dust/gas correlation at high Galactic latitude. *A&A*, 312:256–262, August 1996.

[3] N. R. Hall, R. Keisler, L. Knox, C. L. Reichardt, P. A. R. Ade, K. A. Aird, B. A. Benson, L. E. Bleem, J. E. Carlstrom, C. L. Chang, H.-M. Cho, T. M. Crawford, A. T. Crites, T. de Haan, M. A. Dobbs, E. M. George, N. W. Halverson, G. P. Holder, W. L. Holzapfel, J. D. Hrubes, M. Joy, A. T. Lee, E. M. Leitch, M. Lueker, J. J. McMahon, J. Mehl, S. S. Meyer, J. J. Mohr, T. E. Montroy, S. Padin, T. Plagge, C. Pryke, J. E. Ruhl, K. K. Schaf-

fer, L. Shaw, E. Shirokoff, H. G. Spieler, B. Stalder, Z. Staniszewski, A. A. Stark, E. R. Switzer, K. Vanderlinde, J. D. Vieira, R. Williamson, and O. Zahn. Angular Power Spectra of the Millimeter-wavelength Background Light from Dusty Star-forming Galaxies with the South Pole Telescope. *Astrophys. J.*, 718:632–646, August 2010.

[4] N. R. Hall, L. Knox, C. L. Reichardt, P. A. R. Ade, K. A. Aird, B. A. Benson, L. E. Bleem, J. E. Carlstrom, C. L. Chang, H. -. Cho, T. M. Crawford, A. T. Crites, T. de Haan, M. A. Dobbs, E. M. George, N. W. Halverson, G. P. Holder, W. L. Holzapfel, J. D. Hrubes, M. Joy, R. Keisler, A. T. Lee, E. M. Leitch, M. Lueker, J. J. McMahon, J. Mehl, S. S. Meyer, J. J. Mohr, T. E. Montroy, S. Padin, T. Plagge, C. Pryke, J. E. Ruhl, K. K. Schaffer, L. Shaw, E. Shirokoff, H. G. Spieler, Z. Staniszewski, A. A. Stark, E. R. Switzer, K. Vanderlinde, J. D. Vieira, R. Williamson, and O. Zahn. Angular Power Spectra of the Millimeter Wavelength Background Light from Dusty Star-forming Galaxies with the South Pole Telescope. *Astrophys. J.*, 718:632–646, July 2010.

[5] D. Hanson, S. Hoover, A. Crites, P. A. R. Ade, K. A. Aird, J. E. Austermann, J. A. Beall, A. N. Bender, B. A. Benson, L. E. Bleem, J. J. Bock, J. E. Carlstrom, C. L. Chang, H. C. Chiang, H.-M. Cho, A. Conley, T. M. Crawford, T. de Haan, M. A. Dobbs, W. Everett, J. Gallicchio, J. Gao, E. M. George, N. W. Halverson, N. Harrington, J. W. Henning, G. C. Hilton, G. P. Holder, W. L.

7

Holzapfel, J. D. Hrubes, N. Huang, J. Hubmayr, K. D. Irwin, R. Keisler, L. Knox, A. T. Lee, E. Leitch, D. Li, C. Liang, D. Luong-Van, G. Marsden, J. J. McMahon, J. Mehl, S. S. Meyer, L. Mocanu, T. E. Montroy, T. Natoli, J. P. Nibarger, V. Novosad, S. Padin, C. Pryke, C. L. Reichardt, J. E. Ruhl, B. R. Saliwanchik, J. T. Sayre, K. K. Schaffer, B. Schulz, G. Smecher, A. A. Stark, K. T. Story, C. Tucker, K. Vanderlinde, J. D. Vieira, M. P. Viero, G. Wang, V. Yefremenko, O. Zahn, and M. Zemcov. Detection of B-Mode Polarization in the Cosmic Microwave Background with Data from the South Pole Telescope. *Physical Review Letters*, 111(14):141301, October 2013.

[6] Eric Hivon, Krzysztof M. Górski, C. Barth Netterfield, Brendan P. Crill, Simon Prunet, and Frode Hansen. Master of the cosmic microwave background anisotropy power spectrum: A fast method for statistical analysis of large and complex cosmic microwave background data sets. *The Astrophysical Journal*, 567(1):2, 2002.

[7] A. Lewis and A. Challinor. Weak gravitational lensing of the CMB. *Physics Reports*, 429:1–65, June 2006.

[8] D. N. Limber. The Analysis of Counts of the Extragalactic Nebulae in Terms of a Fluctuating Density Field. *Astrophys. J.*, 117:134, January 1953.

[9] In our analysis, since the fiducial value of r is zero, the derivative of $C_\ell^{\mathrm{BB,res}}$ is non-zero if $\theta_i = r$.

[10] Planck Collaboration, P. A. R. Ade, N. Aghanim, C. Armitage-Caplan, M. Arnaud, M. Ashdown, F. Atrio-Barandela, J. Aumont, C. Baccigalupi, A. J. Banday, and et al. Planck 2013 results. XVIII. The gravitational lensing-infrared background correlation. *A&A*, 571:A18, November 2014.

[11] Planck Collaboration, P. A. R. Ade, N. Aghanim, C. Armitage-Caplan, M. Arnaud, M. Ashdown, F. Atrio-Barandela, J. Aumont, C. Baccigalupi, A. J. Banday, and et al. Planck 2013 results. XXX. Cosmic infrared background measurements and implications for star formation. *A&A*, 571:A30, November 2014.

[12] Planck Collaboration, P. A. R. Ade, N. Aghanim, M. Arnaud, M. Ashdown, J. Aumont, C. Baccigalupi, A. Balbi, A. J. Banday, R. B. Barreiro, and et al. Planck early results. XVIII. The power spectrum of cosmic infrared background anisotropies. *A&A*, 536:A18, December 2011.

[13] Plank Collaboration, P. A. R. Ade, N. Aghanim, M. I. R. Alves, G. Aniano, M. Arnaud, M. Ashdown, J. Aumont, C. Baccigalupi, A. J. Banday, R. B. Barreiro, N. Bartolo, E. Battaner, K. Benabed, A. Benoit-Levy, J.-P. Bernard, M. Bersanelli, P. Bielewicz, A. Bonaldi, L. Bonavera, J. R. Bond, J. Borrill, F. R. Bouchet, F. Boulanger, C. Burigana, R. C. Butler, E. Calabrese, J.-F. Cardoso, A. Catalano, A. Chamballu, H. C. Chi-

ang, P. R. Christensen, D. L. Clements, S. Colombi, L. P. L. Colombo, F. Couchot, B. P. Crill, A. Curto, F. Cuttaia, L. Danese, R. D. Davies, R. J. Davis, P. de Bernardis, A. de Rosa, G. de Zotti, J. Delabrouille, C. Dickinson, J. M. Diego, H. Dole, S. Donzelli, O. Dore, M. Douspis, B. T. Draine, A. Ducout, X. Dupac, G. Efstathiou, F. Elsner, T. A. Ensslin, H. K. Eriksen, E. Falgarone, F. Finelli, O. Forni, M. Frailis, A. A. Fraisse, E. Franceschi, A. Frejsel, S. Galeotta, S. Galli, K. Ganga, T. Ghosh, M. Giard, E. Gjerlow, J. Gonzalez-Nuevo, K. M. Gorski, A. Gregorio, A. Gruppuso, V. Guillet, F. K. Hansen, D. Hanson, D. L. Harrison, S. Henrot-Versille, C. Hernandez-Monteagudo, D. Herranz, S. R. Hildebrandt, E. Hivon, W. A. Holmes, W. Hovest, K. M. Huffenberger, G. Hurier, A. H. Jaffe, T. R. Jaffe, W. C. Jones, E. Keihanen, R. Keskitalo, T. S. Kisner, R. Kneissl, J. Knoche, M. Kunz, H. Kurki-Suonio, G. Lagache, J.-M. Lamarre, A. Lasenby, M. Lattanzi, C. R. Lawrence, R. Leonardi, F. Levrier, M. Liguori, P. B. Lilje, M. Linden-Vornle, M. Lopez-Caniego, P. M. Lubin, J. F. Macias-Perez, B. Maffei, D. Maino, N. Mandolesi, M. Maris, D. J. Marshall, P. G. Martin, E. Martinez-Gonzalez, S. Masi, S. Matarrese, P. Mazzotta, A. Melchiorri, L. Mendes, A. Mennella, M. Migliaccio, M.-A. Miville-Deschenes, A. Moneti, L. Montier, G. Morgante, D. Mortlock, D. Munshi, J. A. Murphy, P. Naselsky, P. Natoli, H. U. Norgaard-Nielsen, D. Novikov, I. Novikov, C. A. Oxborrow, L. Pagano, F. Pajot, R. Paladini, D. Paoletti, F. Pasian, O. Perdereau, L. Perotto, F. Perrotta, V. Pettorino, F. Piacentini, M. Piat, S. Plaszczynski, E. Pointecouteau, G. Polenta, N. Ponthieu, L. Popa, G. W. Pratt, S. Prunet, J.-L. Puget, J. P. Rachen, W. T. Reach, R. Rebolo, M. Reinecke, M. Remazeilles, C. Renault, I. Ristorcelli, G. Rocha, G. Roudier, J. A. Rubio-Martin, B. Rusholme, M. Sandri, D. Santos, D. Scott, L. D. Spencer, V. Stolyarov, R. Sudiwala, R. Sunyaev, D. Sutton, A.-S. Suur-Uski, J.-F. Sygnet, J. A. Tauber, L. Terenzi, L. Toffolatti, M. Tomasi, M. Tristram, M. Tucci, G. Umana, L. Valenziano, J. Valiviita, B. Van Tent, P. Vielva, F. Villa, L. A. Wade, B. D. Wandelt, I. K. Wehus, N. Ysard, D. Yvon, A. Zacchei, and A. Zonca. Planck intermediate results. XXIX. All-sky dust modelling with Planck, IRAS, and WISE observations. *ArXiv e-prints*, September 2014.

[14] B. D. Sherwin and M. Schmittfull. Delensing the CMB with the Cosmic Infrared Background. *ArXiv e-prints*, February 2015.

[15] I. Szapudi, S. Prunet, and S. Colombi. Fast Clustering Analysis of Inhomogeneous Megapixel CMB maps. *ArXiv Astrophysics e-prints*, July 2001.